Research article

Triple band notch compact MIMO antenna with defected ground structure and split ring resonator for wideband applications

Karunakar Patchala [a,b,*], Y. Raja Rao [c], A.M. Prasad [d]

[a] JNTUK, Kakinada, AP, India
[b] EEE Department, P V P Siddhartha Institute of Technology, Vijayawada, AP, India
[c] ECE Department, V R Siddhartha Engineering College, Vijayawada, AP, India
[d] ECE Department, JNTUK, Kakinada, AP, India

A B S T R A C T

A triple band notch multiple-input-multiple-output (MIMO) antenna is designed and proposed with complementary-split-ring-resonators (CSRR) on upper side and defected ground structure on bottom portion of the FR4 substrate material. A square shaped radiating element with cone shaped microstrip line feeding is used in the current design to achieve 50-ohm impedance. A compact dimension of $36 \times 22 \times 1.6$ mm is used to fit this model for portable communication devices. Split ring resonators are placed adjacent to the feed line to improve the gain and defected ground with stubs is placed to enhance the bandwidth characteristics. Proposed antenna has bandwidth ranging from 2 to18 GHz with notching at 5.2–5.8 GHz (WLAN), 11–12 GHz (Satellite Broadcasting) and 12.5–14.5 GHz (Aeronautical Radio Navigation). The envelope correlation coefficient (ECC) is less than 0.005 and mutual coupling is less than 15dB achieved. The prototyped antenna is providing peak realized gain of 5dB and maximum efficiency of 75% in the operating band. The results strongly support the applicability of current antenna model with band notching in wideband communications.

1. Introduction

In recent year's ultra-wideband and broad band systems received significant attention in different communication applications. To avoid the interference associated with narrow band systems like wireless local area network (WLAN), WiMAX, Wi-Fi etc, notching is very much needed. Different notch band techniques are proposed by the researchers in the literature for UWB antennas [1, 2, 3, 4]. To transmit the power efficiently, the channel will play a significant role. The channel capacity needs to be increased without taking additional power and frequency spectrum. This is possible with MIMO technology and the installed multiple antennas should have low coupling between them. Designing MIMO antennas with low coupling is a challenging task to the antenna engineers. Different MIMO antennas are proposed for WLAN, Wi-Fi, UMTS and LTE applications with suitability in portable devices [5, 6, 7, 8]. The studies stating that the MIMO technology in UWB providing better channel capacity over the other with narrow band systems. Various techniques are studied to reduce the coupling in MIMO UWB antennas [9, 10].

The isolation enhancement became challenging task in the design of MIMO antenna. Various decoupling techniques are proposed to reduce the mutual coupling, but the structure occupies more space and made antenna configuration more complex [11, 12]. Diversity antennas are one of the choice to reduce the maximum mutual coupling among the antenna elements. To get out of the interference with existing modern wireless communication systems, filters are required to reject unwanted bands [13, 14]. The band notching characteristics can be achieved by placing slots in the radiating structure, using stubs and split ring resonator slots etc [15, 16, 17]. Recent advancements in MIMO antennas with conformal structures, applications in 5G technology and usage of massive MIMO for advanced communication made significant remark in the technology revolution [19, 20, 21, 22, 23, 24, 25, 26, 27].

In this paper, a compact band notched wideband MIMO model is proposed. The dimension is around $36 \times 22 \times 1.6$ mm on FR4 substrate material with permittivity 4.4. Defected ground structure is used in the design to improve the bandwidth characteristics. To create notch bands, strips are placed on the ground plane. The measured observations are matching with simulation results and good impedance matching with high isolation. The designed antenna with split ring resonators and

---

defected ground structure is showing triple band notch characteristics in the operating band from 2-18 GHz.

2. Antenna geometry

The geometry of the basic MIMO antenna structure to the proposed MIMO antenna model iterations are shown in Figure 1. The basic structure consists of square shaped radiating elements placed on FR4 substrate and pencil point shaped feed line is modelled in such way to attain 50 Ω impedance. The resonant frequency can be calculated from the equation

$$fr = \frac{144}{Lg + Pl + Pg + \frac{A1}{2\Pi Lg\sqrt{\varepsilon_{r\,eff}}} + \frac{A2}{2\Pi P\,l\,\sqrt{\varepsilon_{reff}}}} \qquad (1)$$

L_g' denotes length of ground plane, 'P_L' represents length of the patch and 'P_g' represents gap between them. Here 'A_1' is ground plane area and 'A_2' is patch area. ε_{reff} is the effective dielectric constant and $\varepsilon_{reff} = (\varepsilon r+1)/2$. The L-shaped stub consists of long slot on the structure to provide better isolation between the ports. To attain notching at WLAN band, two strips are added on the ground plane, which behaves like $\lambda/4$ resonators at notch frequency.

$$P_g = L_{f1}+L_{f2}-L_g \qquad (2)$$

To get better isolation between input ports, the long ground is modified as T-shaped ground. Notch bands are created to suppress interference with the help of strip 1 and 2 in T-Shaped ground. They form $\lambda/4$-resonators with two open-end slots and they serve to attain notch frequency. The designed antenna consisting of symmetrical structure, to get identical impedance at two ports.

The gaps in the SRR is providing the magnetic response. The gap in the SRR provides capacitance and with respect to that the equivalent circuit is provided. S-parameters help is taken to model the equivalent circuit for SRR. Ansys HFSS tool with floquent mode is used for analysis and presented in Figure 2(b).
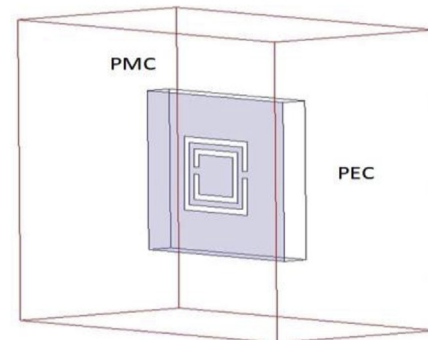
The structure and the parameters of the proposed antenna are presented in Figure 3 and Table 1. The antenna is occupying very compact size of $36 \times 22mm^2$. The split ring resonator dimensions are presented in Figure 2.
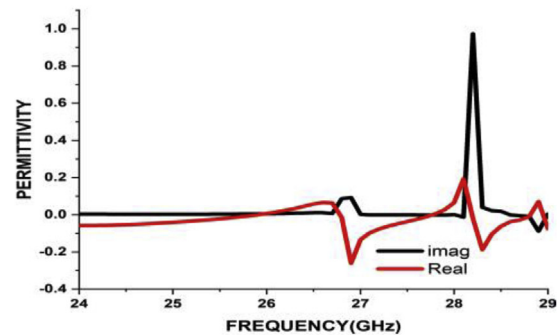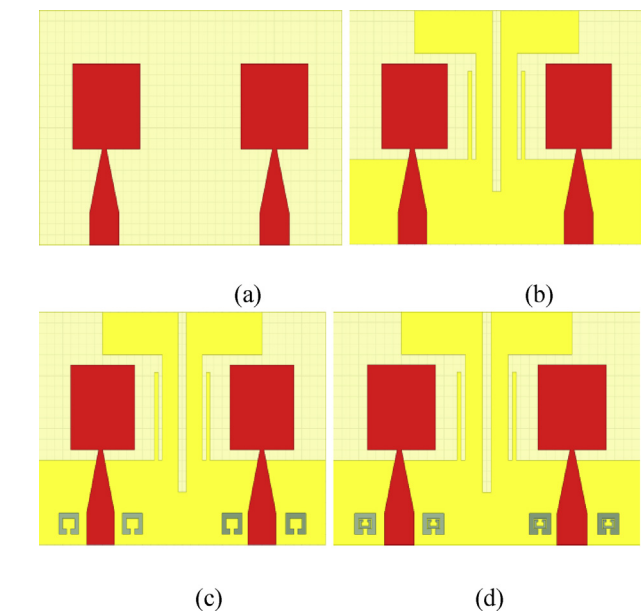

(a)

(b)

(c)

(d)

Figure 2. SRR (a) Split-Ring-Resonator Dimensions, (b) Equivalent Circuit, (c) Port assignment,(d) Permittivity of the SRR.
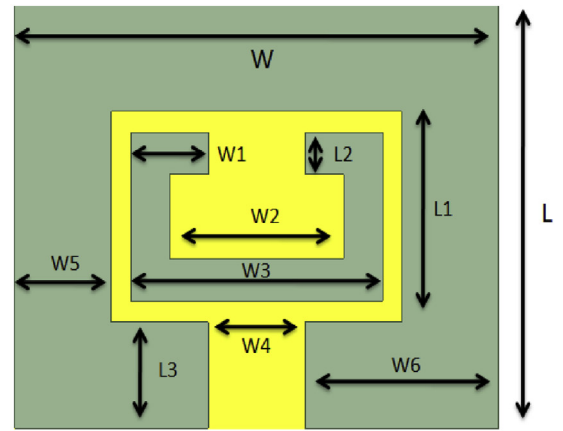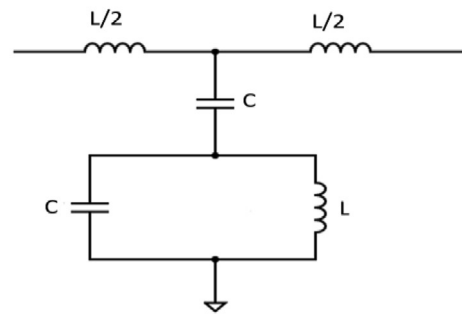
(a)   (b)
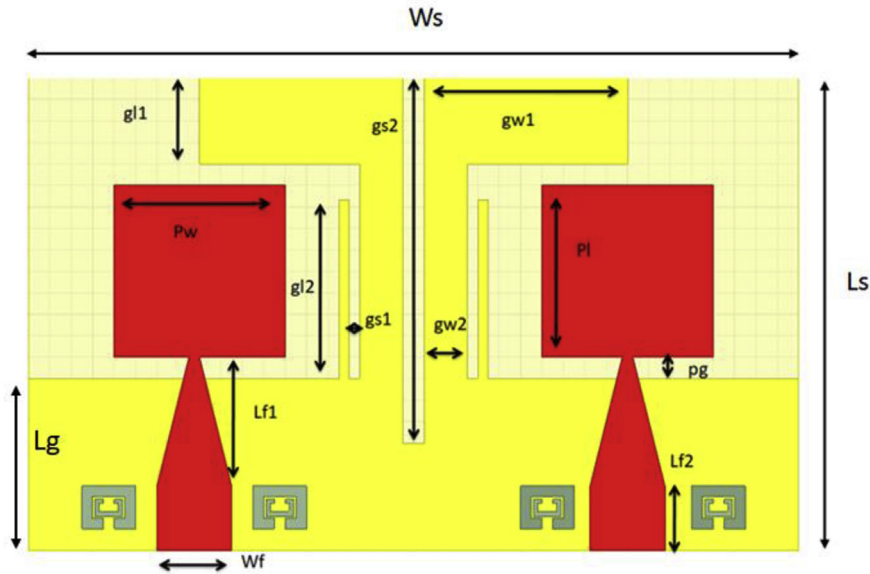
(c)   (d)

Figure 1. MIMO Antenna Iterations, (a) Basic Structure, (b) Antenna Model1, (c) Antenna model2, (d) Proposed antenna.

Figure 3. Proposed SRR based MIMO Antenna.

Table 1. Antenna parameters.

S. No	Parameters	Dimensions in mm	Parameters	Dimensions in mm
1	L_S	22	P_g	1
2	W_S	36	L	2
3	gL_1	4	W	2.4
4	gL_2	8.3	L_1	1
5	gs_1	0.5	L_2	0.2
6	gs_2	18	L_3	0.5
7	gw_1	9.5	W_1	0.4
8	gw_2	2	W_2	0.9
9	P_w	8	W_3	1.3
10	P_l	8.3	W_4	0.5
11	L_{f1}	6	W_5	0.5
12	L_{f2}	3	W_6	1
13	Lg	8	W_f	2.6
14	A1	792	A2	66.4
15	Pi	3.14	ε_{reff}	2.55

Figure 4. Reflection coefficient of designed antenna models.
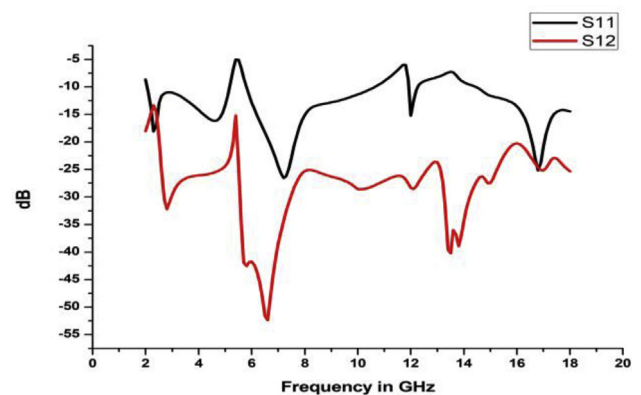
Figure 5. Simulated S_{11} & S_{12} of the proposed MIMO antenna.

3. Results and discussion

3.1. S-parameters

The design of the antenna was simulated by HFSS and the prototyped model results are measured with vector network analyzer (VNA) and antenna measurement setup being in anechoic chamber. When return loss was measured with VNA, a good agreement observed between simulation and measurement. Figure 4 shows the simulated return loss curves for the designed antenna iterations. Antenna model 1(without SRR) and antenna model 2(With SRR) providing dual band notch characteristics at 5.2–5.8 GHz (WLAN) and 11–12 GHz (Satellite Broadcasting) frequency bands. The proposed antenna model with CSRR is providing triple notch band results from 5.2 to 5.8 GHz (WLAN), 11–12 GHz (Satellite Broadcasting) and 12.5–14.5 GHz (Aeronautical Radio Navigation) frequency bands (see Figure 5).

3.2. Effect of ground plane stubs and gap

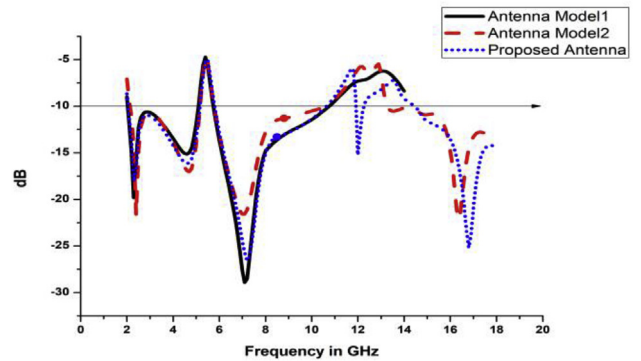The ground consisting of a T-shape of stub to provide good matching to antenna and for the improvement of isolation. This will reflect the radiation from the radiators. The simulation results of VSWR for MIMO antenna with change in T-shaped stub gs$_2$ is presented in Figure 6. When T-shaped stub value is decreasing from 18 to 15mm, there is a significant change in the working band of the MIMO antenna. For gs$_2$ = 18 mm antenna losing its lower operating band and notch band range is also increased.
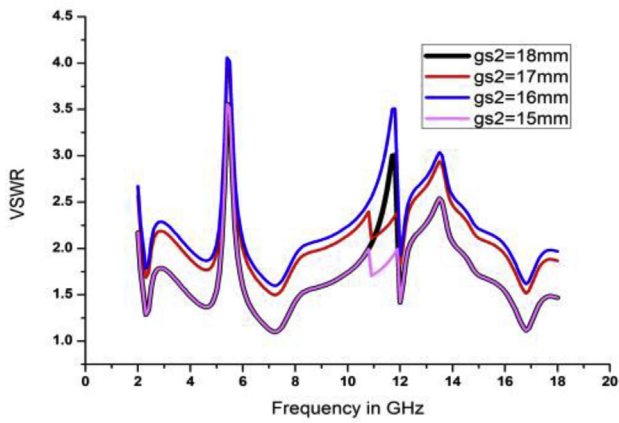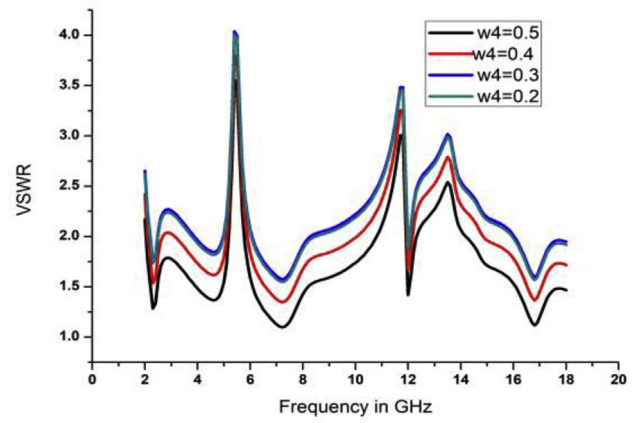
Figure 6. VSWR with change in gs₂.

Figure 8. VSWR with change in w4.

The ground plane stub of gl₂ is varied from 5.3 to 8.3mm and the corresponding VSWR results are plotted in Figure 7. The optimized dimension is 8.3mm, for which the triple notch is obtained and for remaining cases dual notch characteristics are attained. The outer split ring resonator gap 'w₄' is varied and the corresponding VSWR results are exhibited in Figure 8. For the dimension of 0.5 mm gap in the split ring resonator, MIMO antennas providing optimum performance with triple notching. Freq. Vs gain and efficiency plot is presented in Figure 9.

The current distribution plots are used to analyze the effect of isolation in the ground slot. Figures 10 and 11 producing the current distribution of the antenna at 3.6 GHz and 10 GHz respectively. Port1 excited and port2 terminated with 50 Ω. Majority of current is concentrated on the left side to the ground and the coupling to port 2 is very low, which reducing the mutual coupling among the ports. The etched slot in the ground helps to provide good isolation among the ports.
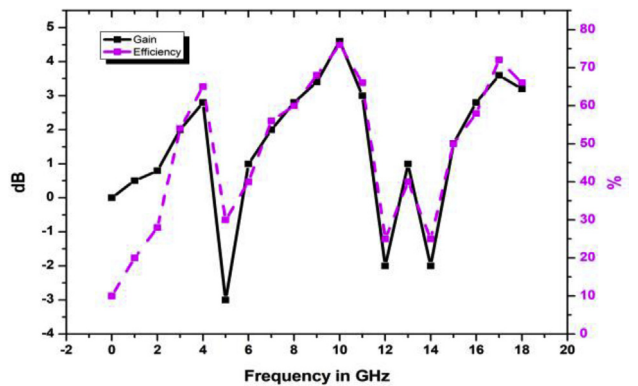
3.3. Radiation patterns

Figures 12, 13, and 14 depicts antenna radiation pattern in three-dimensional view and in polar coordinates. At 3.6 GHz (Wi-Fi band) antenna projecting quasi-omni pattern in the H-field with low cross polarization. A peak observed gain of 3.54 dB is attained at 3.6 GHz and 5.08 dB obtained at 10 GHz. The simulated cross polarization is less than -40 dB and the measured value is little bit greater due to some imperfections in fabrication and nonideal differential signal applied to port in the measurement.
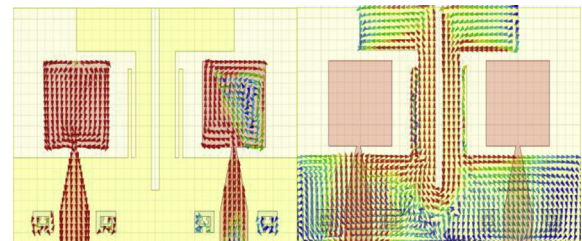

Figure 9. Frequency vs gain and efficiency.

Figure 10. Current distribution at 3.6 GHz, (a) Top side, (b) Bottom side.
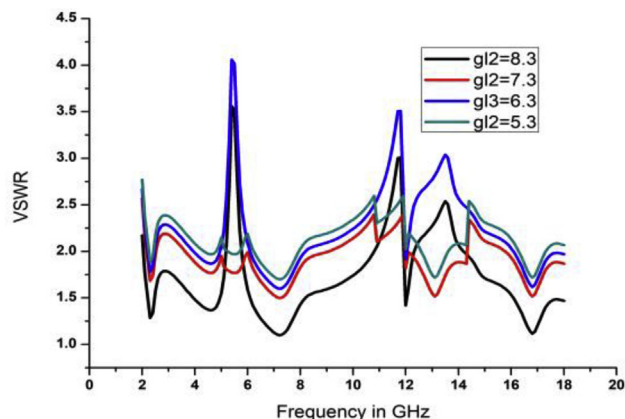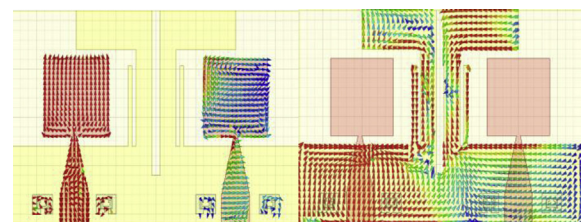

Figure 11. Current distribution at 10 GHz, (a) Top side, (b) Bottom side.

3.4. Envelope correlation coefficient(ECC)

Envelope correlation coefficient(ECC) is the parameter to estimate the performance of diversity in the MIMO antenna. S Blench [18] proposed an equation to determine the ECC from S-parameters. The overlapping between the two radiation patterns can be reduced for the lesser ECC values of the antenna model. The measurement and simulation of
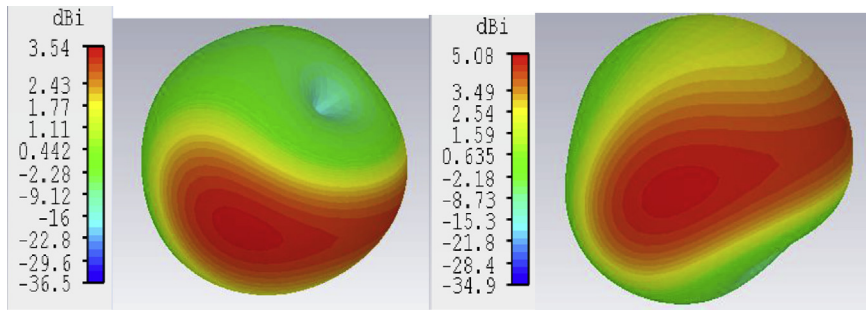

Figure 7. VSWR with change in gl2.

Figure 12. 3D-Radiation pattern with port1 excited and port2 terminated of 50 Ohms at (a) 3.6 GHz and (b) 10 GHz.
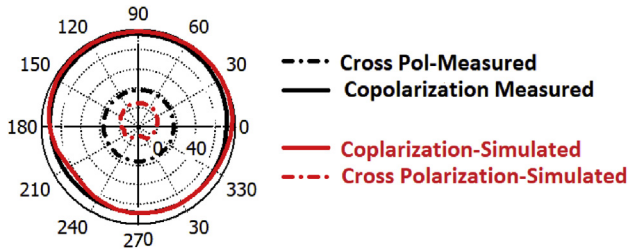

Figure 13. H-Plane Radiation Pattern at 3.6 GHz with port1 excited and port2 terminated with 50 Ohm impedance.
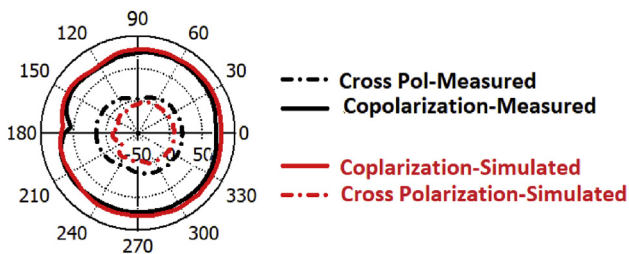

Figure 14. E-Plane Radiation Pattern at 3.6 GHz with port1 excited and port2 terminated with 50 Ohm impedance.

ECC values are plotted in Figure 15. The ECC value of 0.5 is set as acceptable value and in our case except at notch bands the average ECC obtained in the operating band is around 0.001. At notch band the ECC is above 0.003.

The first method to calculate CC is by use of far field radiation pattern for uniform multipath indoor environment formula

$$\rho = \frac{\left| \int \int_{4\pi}^{0} \overrightarrow{F_1}(\theta, \phi) . \overrightarrow{F_2}(\theta, \varphi) d\Omega \right|^2}{\left| \int \int_{4\pi}^{0} \overrightarrow{F_1}(\theta, \varphi) \right|^2 \left| \int \int_{4\pi}^{0} \overrightarrow{F_2}(\theta, \varphi) \right|^2} \tag{3}$$

where $\mathbf{F}_i(\theta, \varphi)$ and $\mathbf{F}_j(\theta, \varphi)$ are named as radiation patterns complex values for the antennas at i and j respectively, when terminated by matched loads for other antennas (usually 50Ω). The operator notation (•) is called as the Hermitian product. In this paper correlation coefficient is taken from the scattering parameters based on the formula

$$\rho_e = \frac{\left| s_{11}^* s_{21} + s_{12}^* s_{22} \right|^2}{(1 - |s_{11}|^2 - |s_{21}|^2)(1 - |s_{22}|^2 - |s_{12}|^2)} \tag{4}$$

3.5. Group delay

The group delay will be measured to identify the error occurred due multiple reflections among the antenna elements. Generally in the MIMO antennas, the group delay will provide information regarding error due to multiple reflections because the elements will be placed nearer to each other. By exciting two identical antennas with placement of face-to-face direction in far field, group delay was noted and presented in Figure 16. In this case when port 1 was excited then port 2 was terminated with 50-ohm impedance and when port 2 was excited then port 1 was terminated with 50-ohm impedance. It is being observed that the measured group delay is flat in the existing band. At notch bands sharp edges are obtained for group delay.

Group Delay G D (f) = - (1 / 360) (dΦ (f) / d f) (5)

where 'G D (f)' is group delay in seconds. 'Φ (f)' is phase function and 'f' represents the frequency.
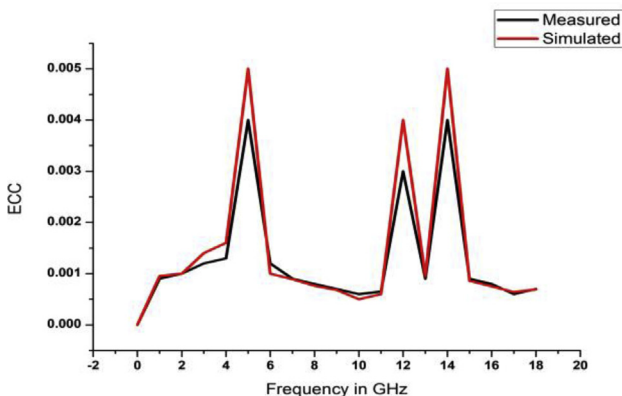

Figure 15. Measurement and simulated Frequency Vs ECC.
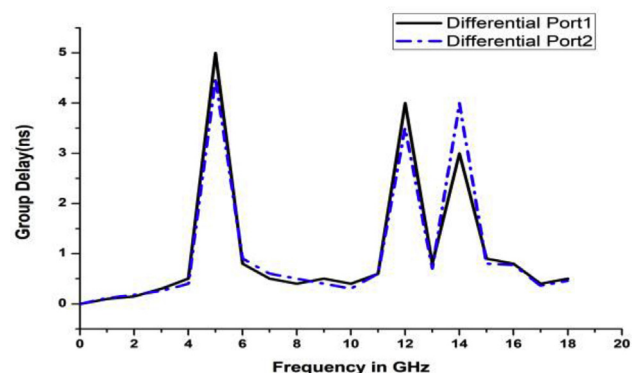

Figure 16. Frequency vs group delay.

3.6. Prototype measurements

The prototyped antenna on FR4 substrate has been shown in Figure 17. The prototyped antenna is analyzed in chamber for the radiation measurement and it can be witnessed from Figure 18. The measured value of reflection coefficient and transmission coefficient along with simulation results are presented in Figure 19.

The current model is compared with the literature and presented in Table 2. As per the peak gain is concerned, the proposed antenna is providing superior gain of 5 dB in the operating band and antenna is capable to notch triple band. The size is little bit high when compared with one or two models, but the performance of the antenna is encouraging for applicability in the desired operations.

3.7. Vehicular placement

Four locations are chosen to mount the antenna on the vehicular body for analysis. Bumper, wind shield glass, rear bumper and side mirror are the locations opted in this measurement.(see Figure 20).

Individual excited elements based mutual coupling is studied and presented the obtained values in Tables 3(a) and 3(b) at 3 GHz. The pointed observations in the Table 3(a) and 3(b) gives the coupling among adjacent neighbor elements (L_n & L_{n+1}) for the locations at A, B, C, & D.

4. Conclusion

A compact MIMO model-based antenna is designed to attain triple notch band characteristics. The designed antenna occupying $36 \times 22 \times 1.6$ mm dimension on FR4 substrate and providing good isolation and impedance bandwidth as per the design requirements. Split ring resonators are placed adjacent to the feed line to improve the gain and defected ground with stubs is placed to enhance the bandwidth characteristics in this current model. Proposed antenna has bandwidth ranging from 2 to18 GHz with notching at 5.2–5.8 GHz (WLAN), 11–12 GHz (Satellite Broadcasting), 12.5–14.5 GHz (Aeronautical Radio Navigation). The current design providing envelope-correlation-coefficient is
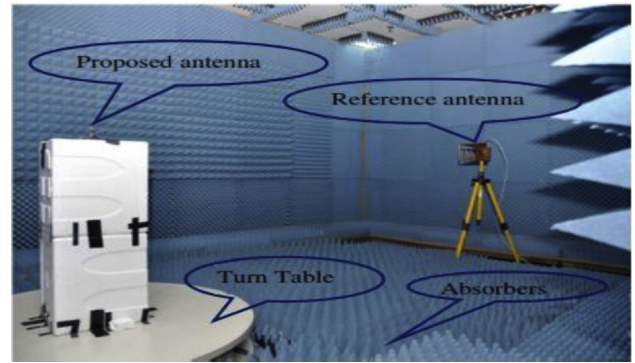
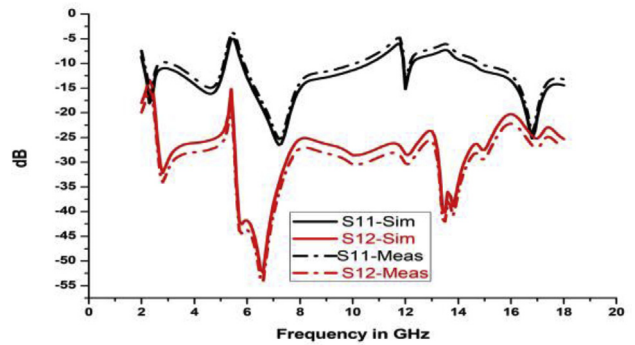

Figure 18. Antenna measurement setup in anechoic chamber.

Figure 19. Simulated & Measured S_{11} & S_{12} of the fabricated antenna.

Table 2. Antenna Model comparison with Literature.

Antenna dimensions	Gain (dB)	Notching band	Ref Paper No
$46 \times 20 \times 1.6$ mm^3	3 dB	Single Band	4
45 mm $\times 45$ mm	3.6 dB	Single Band	6
$29 \times 29 \times 5$ mm^3	2.9 dB	Single Band	14
23×29 mm^2	3.4 dB	Single Band	17
$30 \times 30 \times 1.6$ mm	3 dB	Dual band	1
15×14.5mm^2	3.4 dB	Dual band	2
20 mm $\times 46$ mm	3.8 dB	Dual Band	3
$36 \times 22 \times 1.6$ mm	5 dB	Triple Band	Proposed antenna

lower than 0.08 and mutual coupling lower than 15dB. The prototyped antenna is providing peak realized gain of 5 dB and maximum efficiency of 75% in the working band. The obtained measured results are providing good correlation with simulation results.
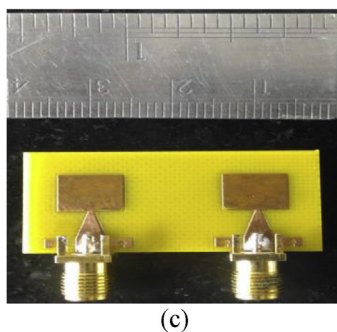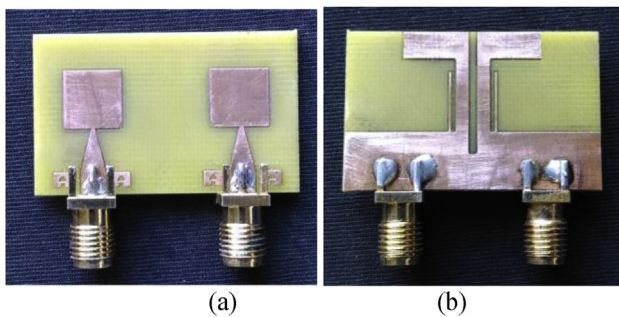

(a)　　　　(b)

(c)

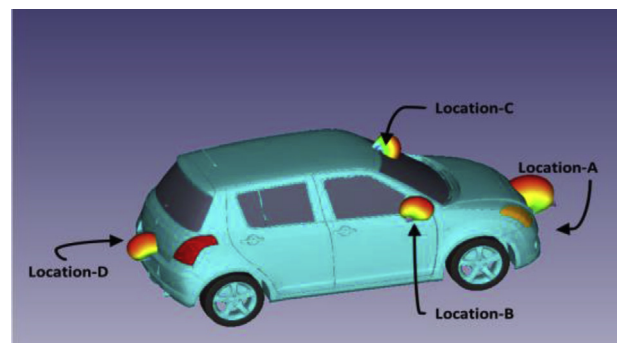**Figure 17.** Designed antenna on FR4 substrate, (a) Top view, (b) Back view, (c) dimensional view.

Figure 20. MIMO antenna placement at specific locations.

Table 3. Coupling characteristics of MIMO antenna at 3 GHz.

	Transmission Antenna			
Reception Antenna	A_1	A_2	B_1	B_2
A_1	NA	-36.093	-85.869	-81.582
A_2	-35.586	NA	-71.667	-73.098
B_1	-76.482	-79.086	NA	-44.195
B_2	-71.232	-73.792	-44.277	NA
C_1	-59.668	-54.736	-61.040	-77.103
C_2	-60.514	-55.328	-69.338	-68.193
D_1	-66.902	-70.280	-74.930	-69.699
D_2	-67.913	-71.346	-74.895	-67.415
Reception Antenna	C_1	C_2	D_1	D_2
A_1	-57.835	-62.634	-70.387	-69.355
A_2	-61.858	-55.93	-70.090	-69.247
B_1	-72.643	-67.317	-67.504	-69.919
B_2	-65.318	-67.929	-69.532	-70.308
C_1	NA	-47.626	-72.230	-72.063
C_2	-43.12	NA	-69.599	-70.151
D_1	-76.846	-69.484	NA	-38.468
D_2	-61.433	-71.888	-38.447	NA

Declarations

Author contribution statement

Karunakar Patchala: Conceived and designed the experiments; Performed the experiments; Wrote the paper.

Y Raja Rao: Conceived and designed the experiments; Analyzed and interpreted the data; Wrote the paper.

A M Prasad: Conceived and designed the experiments; Analyzed and interpreted the data; Contributed reagents, materials, analysis tools or data; Wrote the paper.

Competing interest statement

The authors declare no conflict of interest.

Additional information

No additional information is available for this paper.

References

[1] Zeeshan Ahmed, Gul Perwasha, Ultrawide band antenna with wlan band-notch characteristic, Int Conf Comput, control commun (2013) 25–26.

[2] Noman waheed, Abubakar saadat, Ultra-wide band antenna with wlan and wimax band-notch characteristic, Int Conf Commun, Comput Digital syst 8 (2017).

[3] Shilpa Jangid, Mithilesh kumar, A novel uwb notched rectangular patch antenna with square slot, Inter Conf Comput Intell Commun Netw (2012) 3–5.

[4] Z.Q. Li, C.L. Ruan, A small integrated bluetooth and uwb antenna with wlan band-notched characteristics, Int Symp Signals, Syst Electron 1 (2010) 1–4.

[5] Bo-Ren Hsiao, Yi-An Chen, LTE MIMO Antennas on variable sized Tablet computers with comprehensive Band coverage, IEEE Antennas Wirel. Propag. Lett. 15 (2015) 1152–1155.

[6] Saber Soltani, Parisa Lotfi, A port and frequency reconfigurable MIMO slot antenna for WLAN applications, IEEE Trans. Antennas Propag. 64 (4) (2016) 1209–1217.

[7] Manoj K. Meshram, A novel quad-band diversity antenna for LTE and wi-fi applications with high isolation", IEEE Trans. Antennas Propag. 60 (9) (2012) 4360–4371.

[8] Shrivishal Tripathi, Akhilesh Mohan, Sandeep Yadav, A compact koch fractal UWB MIMO antenna with WLAN band-rejection, IEEE Antennas Wirel. Propag. Lett. 14 (2015) 1565–1568.

[9] Muhammad saeed Khan, Ultra-compact dual polarized UWB MIMO antenna with meandered feeding Lines, IET Microw., Antennas Propag. 11 (7) (2017) 997–1002.

[10] Mohammad Abedian, Compact ultrawide band MIMO dielectric resonator antennas with WLAN band rejection, IET Microw., Antennas Propag. 11 (11) (2017) 1524–1529.

[11] Mohammad mahdi Farahani, Mutual coupling reduction in millimeter-wave MIMO antenna array using a meta material polarization-rotator wall, IEEE Antennas Wirel. Propag. Lett. 16 (2017) 2324–2327.

[12] Mohammad Saeed Khan, A compact CSRR-enabled UWB diversity antenna, IEEE Antennas Wirel. Propag. Lett. 16 (2017) 808–812.

[13] D.S. Ramkiran, B.T.P. Madhav, Sahithi Krishnaveni Grandhi, Amara Venkata Sumanth, Sri Harsha Kota, Leela Krishna Boddu, Compact microstrip band pass filter with defected ground structure", Far East J. Electron. Commun. 15 (1) (2015) 75–84.

[14] P. Lakshmikanth, Kh Takeshore, B.T.P. Madhav, Printed Log Periodic dipole antenna with Notched filter at 2.45 GHz Frequency for wireless communication applications, J. Eng. Appl. Sci. 10 (3) (2015) 40–44.

[15] Wing-xin chu, Compact broad band slot MIMO antenna with a stub loaded radiator, IEEE conference on Antenna Measurements and Applications (2014) 1–4.

[16] Ashok Kumar, Mahindra Mohan Sharma, A compact triple-band planar mimo diversity antenna for wi max/wlan applications, Inter Conf Comput, Commun Electron (2017) 236–240.

[17] J. Chandrasekhar Rao, N. Venkateswara Rao, Compact UWB MIMO slot antenna with defected ground structure, ARPN J Eng Appl Sci 11 (17) (2016).

[18] S. Blanch, J. Romeu, Exact representation of antenna system diversity performance from input parameter description, Electron. Lett. 39 (9) (2003) 705–707.

[19] B.T.P. Madhav, Defected ground structured compact mimo antenna with low mutual coupling for automotive communications, Microw. Opt. Technol. Lett. (2018) 1–7.

[20] G. Jyothsna Devi, P. Lakshman, A CPW-fed sigma-shaped MIMO antenna for ka band and 5G communication applications, J Telecommun Inf Technol 4 (2018) 1–8.

[21] Y. Usha Devi, Conformal printed MIMO antenna with DGS for millimeter wave communication applications, Int Electron Lett (2019).

[22] M. Venkateswara Rao, CSRR-loaded T-shaped MIMO antenna for 5G cellular networks and vehicular communications, Int. J. RF Microw. Computer-Aided Eng. (2019).

[23] H. Huang, X. Li, Y. Liu, A low-profile, dual-polarized patch antenna for 5g mimo application, IEEE Trans. Antennas Propag. 67 (2) (2019) 1275–1279.

[24] Mohammad Akbari, Hamdan abo ghalyon, Mohammadmahdi farahani, Abdelrazik sebak, A. Tayeb, Denidni. Spatially decoupling of CP antennas based on FSS for 30-GHz MIMO systems, IEEE Access 5 (2017) 6527–6537.

[25] D. Piao, Y. Wang, Tri-polarized MIMO antenna using a compact single-layer microstrip patch, IEEE Trans Antennas Propag (2018).

[26] M. Farahani, J. Pourahmadazar, M. Akbari, M. Nedil, A.R. Sebak, T.A. Denidni, Mutual coupling reduction in millimeter-wave MIMO antenna array using a metamaterial polarization-rotator wall, IEEE Antennas Wirel. Propag. Lett. 16 (2017) 2324–2327.

[27] S. Asaad, A.M. Rabiei, R.R. Müller, Massive MIMO with antenna selection: fundamental limits and applications, IEEE Trans. Wirel. Commun. 17 (12) (2018) 8502–8516.